

# Monitoring soil moisture dynamics in multilayered Fluvisols



József Dezső<sup>1</sup>, Szabolcs Czigány<sup>1</sup>, Gábor Nagy<sup>1,\*</sup>, Ervin Pirkhoffer<sup>1</sup>, Marcin Słowik<sup>2</sup>, Dénes Lóczy<sup>1</sup>

<sup>1</sup> University of Pécs, Institute of Geography and Earth Sciences, Faculty of Sciences, Hungary

<sup>2</sup> Adam Mickiewicz University, Faculty of Geographical and Geological Sciences, Poland

\* Correspondence: <sup>1</sup>University of Pécs, Institute of Geography and Earth Sciences, Faculty of Sciences, H-7624 Pécs, Ifjúság útja 6. Hungary. E-mail: [gnagy@gamma.ttk.pte.hu](mailto:gnagy@gamma.ttk.pte.hu)

 <https://orcid.org/0000-0002-9158-3162>

**Abstract.** The identification of drought-sensitive areas (DSAs) in floodplain Fluvisols of high textural pedodiversity is crucial for sustainable land management purposes. During extended drought periods moisture replenishment is only available by capillary rise from the groundwater. However, moisture flux is often hindered by capillary barriers in the interface between layers of contrasting textures. The results of HYDRUS-1D simulations run on multilayered soil profiles were integrated into textural maps to determine the spatial distribution of water dynamics on the floodplain of the Drava River (SW Hungary). Model runs and field data revealed limited moisture replenishment by capillary rise when both contrasting textural interfaces and sandy layers are present in the profile. By implementing these textural and hydraulic relations, a drought vulnerability map (DSA map) of the operational area of the Old Drava Programme (ODP) was developed. According to the spatial distribution of soils of reduced capillary rise, 52% of the ODP area is likely threatened by droughts. Our model results are adaptable for optimisation of land- and water-management practices along the floodplains of low-energy and medium-sized rivers under humid continental and maritime climates.

**Key words:**  
 floodplain pedodiversity,  
 water balance monitoring,  
 drought hazard,  
 infiltration,  
 HYDRUS-1D

## Introduction

Riverine ecosystems are under great pressure from human land use, pollution and resource exploitation (European Parliament 2008; Hulisz et al. 2015; Karasiewicz et al. 2017). Soil texture and profile textural heterogeneity may significantly influence soil hydraulic properties (Li et al. 2013). Floodplain vadose-zone hydraulic processes are driven by dry and extreme wet spells and episodic floods and droughts (Colloff and Baldwin 2010). Water gains and losses vary significantly with the types and locations of soils in often dangerously desiccating floodplains (Lóczy 2019). The resilience along the length of the

floodplain ecosystem, however, can be significantly decreased by human disturbances. Drought conditions can be further exacerbated by the incision and entrenchment of regulated rivers (Burián et al. 2019).

Floodplains, which often have high pedodiversity, typically display unique alluvial layering with various, but identifiable, soil texture and known hydraulic behaviour (Vereecken et al. 2016). The spatiotemporal variability of soil moisture and water availability depends on multiple environmental factors, including topography, layering of fluvial deposits (Słowik et al. 2018), soil texture, land use, elevation, soil depth and root concentration. If detailed geomorphological and soil texture maps and

data are available, areas with high drought-hazard potential can be determined with field monitoring and hydrologic models at a resolution of a few hectares.

Although droughts must have been common in earlier times, the available archival data on severe water conditions is too limited (Kiss and Nikolić 2015). Water stress and intensification of drought hazard in the studied area of the Drava River's floodplain in SW Hungary is influenced by several factors. The recent incision and entrenchment of the Drava River led to groundwater tables dropping by 1.5–2.5 metres and an increasing water shortage (Lóczy et al. 2017; Dezső et al. 2018; Burián et al. 2019). The resilience of the floodplain was further depleted by river regulation works and the implementation of flood control strategies. Due to profound human interventions (enhanced water retention in the hydroelectric dams in the Croatian reach, construction of levees, gravel extraction from the riverbed) mean water stages have been decreasing in the river (Burián et al. 2019). Therefore, low water stages have been observed for a longer duration over recent years, lowering the groundwater table. The water shortage is also due to the aridification trend related to global climate change (Lóczy et al. 2019). The flood retention role of the wetlands of the Danube–Drava National Park in the floodplain has also lost its resilience due to the shrinking water surfaces of oxbow lakes (Lóczy et al. 2019).

Although the floodplain of the Drava River is apparently flat, the physical properties of soil are controlled by ridge-and-swale topography (Hickin 1974; Leclerc and Hickin 1997; Gibling and Rust 2009). According to our field observations and satellite images, soil surface properties have changed at a scale of a few tens of metres. Crop growth and yield varies in bands of a 10- to 30-metre width, which corresponds with the horizontal fluviomorphological structures of point bars (Lieb and Sulzer 2019). The mosaic pattern of floodplain Entisols (WRB: Fluvisols) involves extreme water conditions both spatially (contrasts in moisture contents between landforms of minimal difference in elevation) and temporally (excess and ponding water in spring, and extreme droughts in late summer). As a consequence, significant variations in agricultural productivity and crop yields are observable spatially and inter-annually.

Crops with shallow rhizospheres may experience water stress and extreme drought in years of low precipitation at and below the permanent wilting point (PWP) while overly rainy growing seasons' excess ponding water and anoxic conditions in the vadose zone may cause considerable yield losses (Lizaso and Ritchie 1997; Vogt and Somma 2013; FAO 2012). The matric potential at the PWP is commonly estimated at -15 bar. Most agricultural plants will generally show signs of wilting long before this moisture potential or water content is reached ( $PWP_{\text{field}}$ , more typically at around of -2,000 to -5,000  $H_2O$ -cm) because the rate of water movement to the roots decreases and the stomata tend to lose their turgor pressure and begin to restrict transpiration. This water is strongly retained and trapped in the smaller pores, and does not readily flow.

Surface and subsurface waters of floodplains form a single system where the crucial components are linked by infiltration, capillary rise, soil moisture and groundwater flow in models (Winter et al. 1999; Rajkai et al. 2015; Arkhangel'skaya et al. 2016; Mohawesh et al. 2017). However, soil profiles that include a capillary barrier likely limit the upward moisture movement. The rationale behind this is that layering with contrasting textural changes significantly hinders upward vertical flux, i.e. replenishment by capillary rise (Huang et al. 2011). Other studies, however, indicated an increase in the water budget of the vadose zone. These contradictory results may be rooted in the uncertainties in water dynamics. Water dynamics and water retention curves can be obtained from arduous measurements (Várallyay és Rajkai 1987), pedotransfer functions (Rajkai and Kabos 1999; Makó et al. 2010; Tóth et al. 2015; Karup et al. 2016; Gohardoust et al. 2017) or numeric models, e.g. the RETention Curve computer program (RETC) (van Genuchten et al. 1991). In spite of major progress over recent decades, models of soil processes are seldom related to the delivery of ecosystem services (Vereecken et al. 2016; Mamedov et al. 2017). Therefore, our specific goals were the following:

1. To reveal the water dynamics of the study area by monitoring moisture content, tension and flux changes of two profiles representative for the Hungarian bank of the Drava floodplain.

2. To verify whether soil profiles with a multilayered character can retain more water than homogeneous profiles, as suggested by previous studies, and whether the presence of capillary barriers therefore results in depleted soil moisture contents in the rooting zone.
3. To determine whether capillary rise can compensate moisture shortage in the root zone (upper 25 cm) of the soil at the study site: according to our hypothesis, capillary rise contributes to reducing water stress and drought hazard in the root zone.
4. To provide additional textural details at a spatial resolution of microregional scale (a few tens of metres) for the existing soil textural map (AGROTOPO, Várallyay et al. 1979, 1980) in respect of its regional and site-specific re-evaluation and upgrade.
5. To generate and delineate a more sophisticated textural and hydrodynamical map of drought-sensitive areas (DSA) within the study site to achieve more applicable spatial information for stakeholders in the efficient management of land and water.

## 2. Methods

### 2.1. Study area

The studied area is the operational area of the Old Drava Programme (ODP, Lóczy and Dezső 2019) that dates back to 2007 and began to be implemented in 2012. The area covers a land surface of 572.14 km<sup>2</sup> and is located in SW Hungary in the floodplain of the Drava River (Fig. 1), where ridge-and-swale topography determines the spatial distribution of soil texture types and pedodiversity. The studied area has a humid continental climate with a mean annual temperature of 11.0°C (1981 to 2010) and a mean annual precipitation total of 680 mm with late-spring and early-summer precipitation dominance. The primary land use is arable land with the dominance of dryland crops typical of humid continental climates, such as corn, wheat, sunflower, soy bean and sugar beet and various crops grown in horticultures, e.g. green pepper, water melon, to-

mato and cucumber. Wetland habitats are found in local depressions and backswamps, where reforestation is often inhibited by falling groundwater tables.

### 2.2. Characterisation of morphological heterogeneity and textural diversity of the studied area

The soils of the study area are generally Fluvisols of various characters. The soil type of Cún-1 is Entisols (suborder: Arents) according to Soil Taxonomy, and Haplic Fluvisol (Siltic, Orthoarenic) according to the World Reference Base for Soil Resources (IUSS Working Group, WRB 2015) classification. Cún-2 was also characterised by Entisols (suborder: Psamments) and Histic Fluvisol (Orthosiltic, Orthoarenic, Endoclayic) according to the Soil Taxonomy and WRB classification systems, respectively.

Soil samples were taken at 88 sampling sites (Fig. 1c) by hand augering to a depth of 120 cm. Soil samples were taken for the depths of 0 to 20 cm, 20 to 60 cm and 60 to 120 cm and, in respect to their texture, were considered representative for these depth ranges. Samples were then taken to the laboratory and were oven dried at 60°C until they reached a constant weight.

### 2.3. Field water balance monitoring

Two hydrometeorological monitoring stations, Cún-1 and Cún-2, were installed on July 25 and August 8, 2013, respectively (Fig. 1). Each station included an infiltrometer (Drain Gauge G2 Passive Capillary Lysimeter), two water potential sensors (MPS-2) and two soil moisture sensors (5TM). Moisture and tension ( $h$ ) values were monitored at depths of 25 cm and 70 cm. Vertical flux directions (upward or downward) were calculated based on the difference between the tension values at depths of 70 and 25 cm ( $h_{70\text{ cm}} - h_{25\text{ cm}}$ ). This means that negative values indicate infiltration, while positive values show capillary rise. Precipitation was measured with an ECRN-100 tipping-bucket rain gauge (resolution of 0.2 mm) in the village of Szaporca, located about 2 km from the monitoring sites (all sensors manufactured by Decagon Devices Inc., Pullman, WA,

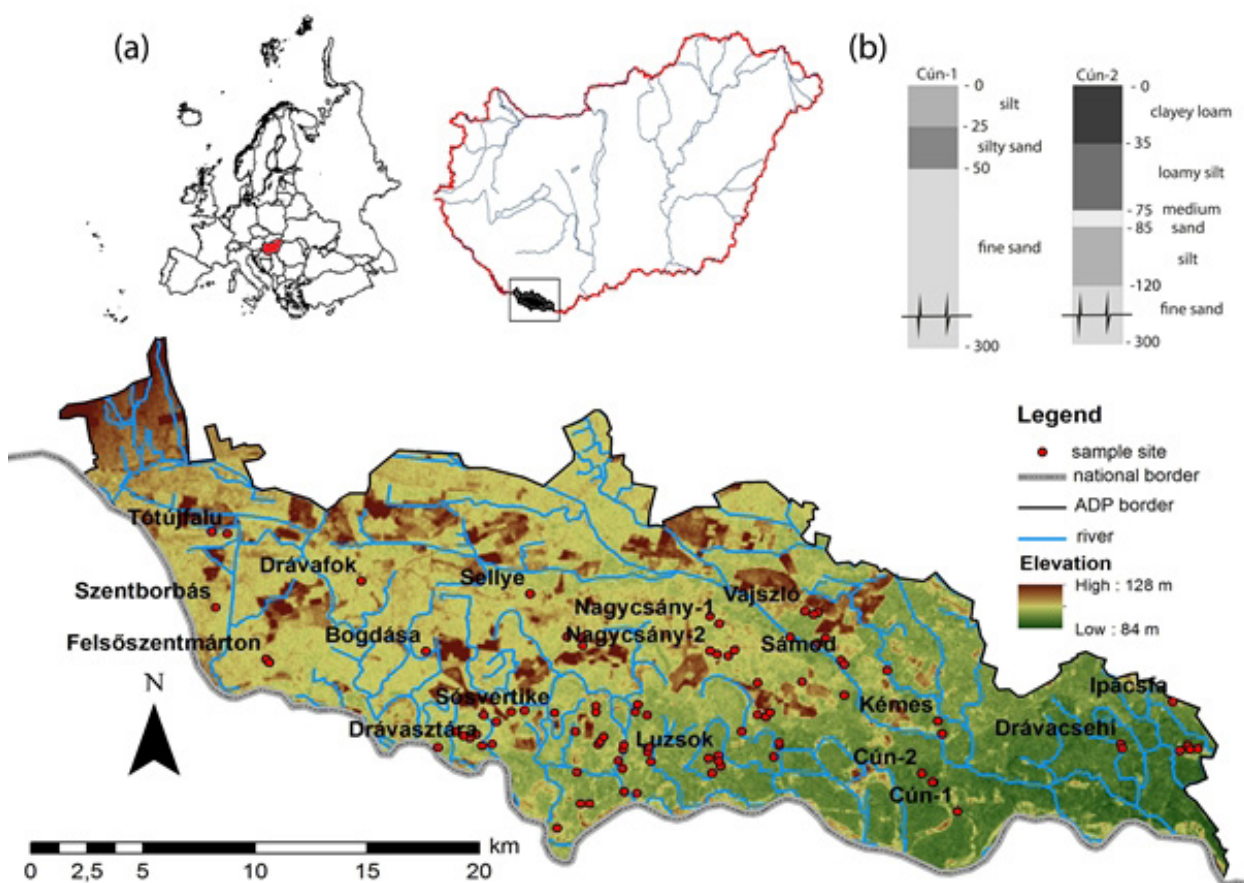


Fig. 1. Location of the stations providing the data used in the article

USA). Data logging was done with Decagon (now called Meter Group) EM50 dataloggers in 30-minute intervals for all subsurface measurements and 10-minute intervals for rainfall measurements. Field monitoring was terminated on June 4, 2014. Measurement series were interrupted for technical reasons (corrosion of instruments, data loss for soil moisture at 25 cm depth at Cún-2 in April, 2014). Groundwater table depth was monitored with Dataqua LB 601 pressure sensors (Dataqua Co., Balatonalmádi, Hungary).

## 2.4. Laboratory analyses

Particle size distribution was determined for three depths (10, 40 and 90 cm) for all 88 study sites and then soil samples were classified texturally according to the five textural classes of the AGROTOPO database. Particle size analyses were performed with a Malvern MasterSizer 3000HS (Malvern Inc., Mal-

vern, England, United Kingdom) particle size analyzer. Samples were pre-treated with HCl and H<sub>2</sub>O<sub>2</sub> for the removal of CaCO<sub>3</sub> and organic matter, respectively.

To obtain water retention curves (WRCs) nine undisturbed soil samples in brass rings of 250 cm<sup>3</sup> and 98 mm in diameter, representative for the textural classes of the study site, were collected in three repetitions in the field to generate WRCs. The average of the three WRCs was then used in the HYDRUS simulations. The bulk and particle densities of the soil types were determined using the methods of Grossman and Reinsch (2002) and Flint and Flint (2002), respectively.

For the determination of the drying curve of the WRCs, soil samples were initially saturated with water and then placed on a hotplate at a temperature of 60°C. Water loss from the brass rings was measured on a laboratory scale (resolution of 0.01 g), while water potential was measured with Decagon MPS-2 sensors. Measurements were done un-

til the water potential fell below permanent wilting point (PWP) or reached a relatively constant weight.

## 2.5. Modelling in RETC and HYDRUS-1D

### Modelling of WRCs in RETC

Modelling of soil moisture content was carried out using the van Genuchten–Mualem equation. The water retention curve model by Mualem (1976) and van Genuchten et al. (1980) calculates unsaturated hydraulic conductivity  $K(h)$  from

$$K(h) = K_s S_e^I \left[ 1 - \left( 1 - S_e^{\frac{1}{m}} \right)^2 \right]^2 \quad (1)$$

where  $K_s$  is the saturated hydraulic conductivity ( $L T^{-1}$ ),  $S_e$  is the effective saturation ( $m^3 m^{-3}$ ), and  $I$  is the tortuosity parameter in the conductivity function, while  $m$  can be calculated as  $m = 1 - 1/n$ . The effective saturation ( $S_e$ ) is calculated as follows (van Genuchten et al. 1980):

$$S_e = \frac{1}{(1 + |\alpha h|^n)^m} \quad (2)$$

where  $\alpha$ , is the inverse of the air entry pressure; and  $n$  and  $m$  are fitting parameters in the van Genuchten–Mualem equation. The model’s fitting parameters are then used as texture-specific input parameters for subsurface flow models, like HYDRUS-1D (Šimůnek et al. 2008; Šimůnek et al. 2016). The van Genuchten soil hydraulic parameters were estimated with the RETC software (v.6.02) using the van Genuchten–Mualem equation (Mualem 1976; van Genuchten et al. 1991) by fitting retention data,  $\theta(h)$  (water retention curve, drying curve only).

$$\theta(h) = \frac{\theta_s - \theta_r}{(1 + |\alpha h|^n)^m} + \theta_r \quad [3]$$

where  $\theta_h$  is the volumetric water content [ $L^3 L^{-3}$ ] at pressure head  $h$ ,  $\theta_r$  is the residual water content [ $L^3 L^{-3}$ ],  $\alpha$  is a parameter related to the inverse of the air entry suction,  $h$  is the suction pressure ( $H_2O$ -cm) and  $n$  is a measure of the pore-size distribution, and  $m = 1 - 1/n$ .  $\theta_s$  (saturated water content, [ $L^3 L^{-3}$ ]).  $K_s$  were measured under laboratory conditions. Data were fitted using the water retention curves obtained from laboratory measurements described in the subchapter “Field water balance monitoring”.

WRCs were generated and RETC simulations were run for nine textural soil types that partly overlapped with the USDA and the 11-class Hungarian textural triangle. Soils were then reclassified for subsequent mapping into five dominant textural types (clay, clay loam, loam, sandy loam and sand) for the harmonisation with the five textural classes of the Hungarian AGROTOPO soil database (Table 1). The reason for the reduction of nine soil types to five was that the AGROTOPO Hungarian soil database only contains the aforementioned five soil types. Textural harmonisation of this sort has yielded satisfactory spatial correlations between the 12 soil types of the USDA textural triangle and the five types of the AGROTOPO database (Pirkhoffer et al. 2006).

The van Genuchten–Mualem hydraulic parameters obtained during the RETC simulations were then used in the HYDRUS-1D simulation runs. However, instead of the nine soil textural types, the obtained soil hydraulic parameters ( $\alpha$ ,  $n$  and  $K_s$ ) were only used for five soil types (sand, loamy sand, loam, clay loam and clay) in the HYDRUS-1 simulation runs.

A second method for the estimation and calibration of hydraulic parameters ( $\alpha$ ,  $n$  and  $K_s$ ) was the use of the one-dimensional HYDRUS-1D (4.16.0110) computer program (Šimůnek et al. 2008) for the Cún-1 and Cún-2 profiles and a theoretical multilayered profile (TML), which was the most common profile horizonation sequence among the 88 drilling sites. The theoretical model was built up of silty sand to a depth of 25 cm from the ground surface, loamy sand for a depth of 25 to 50 cm and clay loam at a depth of 50 to 320 cm (profile Cún-1 served as a template).

The field-measured infiltration rates, pressure heads and soil moisture contents at depths of 25 and 70 cm were used to further calibrate, control and fine-tune the van Genuchten parameters using an inverse solution in HYDRUS-1D. Among the input hydraulic parameters, porosity and saturated water content ( $\theta_s$ ), and  $\theta_r$ , as well as  $K_s$ , were measured in the laboratory;  $\alpha$ ,  $n$  and  $m$  were calculated in RETC and were adjusted with the inverse simulations.

### Forward modelling of soil moisture

The HYDRUS-1D software was also selected to simulate water dynamics for the Cún-1, Cún-2 and the TML profiles at three daily evapotranspiration rates (3, 5 and 7 cm d<sup>-1</sup>) and initial tension gradient scenarios. To simulate the temporal changes of tension at depths of 5, 10, 15 and 20 cm, simulation periods of 30 days were modelled in HYDRUS-1D (Fig. 2). Although extremely dry weather without rainfall over a period of 30 days is rather extreme in Hungary, such conditions are predicted by the REMO and ALADIN models for the future for the lowlands of the country, especially in its southern and south-eastern part (Blanka et al. 2013).

Daily evapotranspiration rates of 3 and 5 mm d<sup>-1</sup> are common values in Hungary during the summer months, but 7 mm d<sup>-1</sup> is extreme and a worst-case scenario assuming a mean daily temperature of 30°C based on the outputs of the Thornthwaite equation (Thornthwaite 1948) for the Drava Floodplain. Model runs in forward mode were parameterised at initial surface pressures of (i) -330 H<sub>2</sub>O-cm and (ii) -4,000 H<sub>2</sub>O-cm with a gradual gradient to a depth of 320 cm (mean groundwater table depth). An initial tension of -4,000 H<sub>2</sub>O-cm was selected to study the effect of capillarity on the replenishment of the vadose zone. A water-stress threshold value of -2,000 was selected for the initial conditions of -330 H<sub>2</sub>O-cm, when initial tension was at -4,000 H<sub>2</sub>O-cm the conventional PWP of -15,000 H<sub>2</sub>O-cm was used.

If an initial tension of less than -4,000 H<sub>2</sub>O-cm was used in the model runs, HYDRUS-1D failed to

execute the simulations. The upper boundary condition (BC) was set to “atmospheric BC with surface layer,  $h_{max}$  at surface = 0 cm”, while the lower boundary was fixed to “constant pressure head” at the depth of the mean groundwater table. For all simulation scenarios, groundwater table depth was fixed at 320 cm. Observation depths were set to 5, 10, 15 and 20 cm, which correspond with the depth of the highest density of roots for the crops grown in the study area (wheat, corn, sunflower, sugar beet and soy). We assumed no precipitation for the 30-day modelling period. The effect of hysteresis was not activated in the simulations, while vapour and heat transport and root uptake were all enabled.

Water stress for crops grown in the area (corn, wheat, sunflower, beetroot, soy, and horticulture plants such as tomato, green pepper, water melon and cucumber) were assumed at and below the field PWP value of -2,000 H<sub>2</sub>O-cm.

### Determination of the spatial distribution of DSAs and the development of the DSA map

The profile layering of the 88 sampling sites served as a basis for the upscaling procedure, and also for the determination of the drought sensitive areas (DSAs) based on HYDRUS-1D model runs. We generated three textural maps for the depths of 0–20 cm, 20–60 cm and 60–120 cm, based on the data obtained by field sampling. By determining the existence of horizons of sandy texture and the presence of textural boundaries with contrasting horizons of the three maps, we generated the drought-sensitivity map of the area, called the “DSA

Table 1. Textural harmonisation between the USDA textural triangle classes and the AGROTOPO textural classes

Textural classes used for the generation of the WRCs	AGROTOPO textural classes
Heavy clay	
Clay	Clay
Clay loam	Clay loam
Sandy loam	
Loam	Loam
Silt loam	
Sandy loam	
Loamy sand	Sandy loam
Sand	Sand

Inverse modelling of soil moisture

map”. Polygons of high drought vulnerability in the DSA map include both contrasting textural horizon boundaries and at least one layer of sandy texture among the three layers of the textural maps.

### 3. Results and Discussion

#### 3.1. Results of the field monitoring

The studied period (duration: 9 months and 21 days) had higher total rainfall than the long-term annual average of the area (680 mm). Total rainfall reached 1,014 mm for the period between August 15, 2013 and June 4, 2014 in the village of Kémes.

In respect of its textural horization profile, Cún-2 differed markedly from Cún-1, as profile Cún-2 is built up of five layers of different textures (loam, silt sand, loam and sand from the top to the bottom). It contained a layer of coarse sand of 10 cm thickness (between the depths of 75 and 85 cm) which distinctly influenced local moisture dynam-

ics and presented a capillary barrier to the adjacent layers.

Soil moisture values for the depth of 25 cm of the Cún-1 profile ranged between 12.8 and 25.6% over the monitored period. These values were higher than those measured at a depth of 70 cm (6.9 to 15.7%) (Fig. 1b). This inverse behaviour of soil moisture as a function of depth is explained by the vertical textural differences in the profile, as a silty topsoil of 25 cm overlay a silty sand layer. Due to the coarser texture in the profile below the depth of 25 cm, there was limited capillary rise in the deeper part of the profile (fine sand, Fig. 1b).

Over the studied period, the Cún-2 profile had a higher infiltration rate and retention capacity. This result is likely explained by the multilayered character of profile Cún-2 and corresponds well with former results (e.g. Bruch 1993; Si et al. 2011; Li et al. 2013). Water recharge and replenishment, which are confirmed by field monitoring, dominated the vadose zone in autumn, winter and spring at the Cún-2 site. Total cumulative infiltration was higher for profile Cún-2 (605 mm) than for Cún-1 (530 mm) over the monitored period, likely due to the

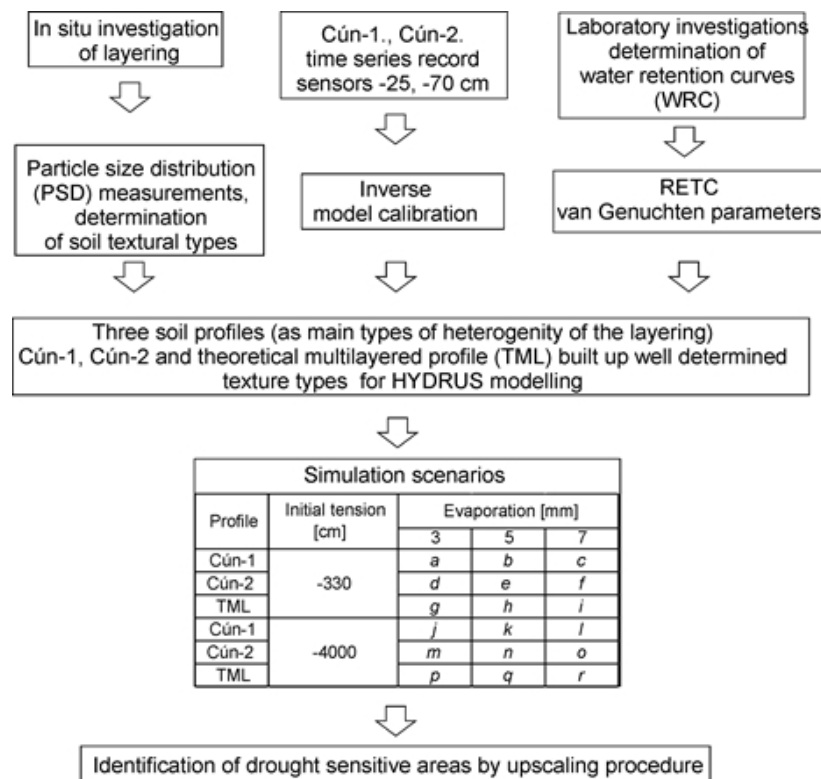


Fig. 2. Flow chart diagram of the analytical procedures during the current study

overall coarser particle fractions. Prolonged and relatively consistent infiltration events were observed in the winter season, especially for profile Cún-2, while only short infiltration events with occasional high peaks were detected in late spring and early autumn (Fig. 3).

Vertical unsaturated and saturated flow directions (Fig. 3d) predominantly indicated infiltration (negative values) while capillary rise (positive values) was only observed for summer, early autumn and April (the driest month) for the Cún-2 profile. Water recharge and replenishment by rainfall, which were confirmed by field monitoring, dominated the vadose zone in autumn, winter and spring at the Cún-2 site. During the second half of August and most of September of 2013, and April of 2014 moisture content of the vadose was replenished by capillary rise for profile Cún-2 (Fig. 3d). Capillary rise dominated flux in profile Cún-1 in August, 2013 and April, 2014. The pronounced late-September infiltration peak was caused by the lag of infiltration and soil moisture response between the depths of 25 and 70 cm (Fig. 3b).

### 3.2. Inverse HYDRUS modelling

The HYDRUS-1D model was used to simulate pressure heads for the Cún-1 and Cún-2 soil profiles. For the verification of the model and inverse modelling of monitored data, both tension and soil moisture data were simulated. Correlations between the monitored and modelled data were  $p=0.984$  and  $p=0.841$  for profiles Cún-1 and Cún-2, respectively. The root of mean square error between modelled and measured data was 0.026 and 0.014 for Cún-1 and Cún-2, respectively.

### 3.3. Forward Simulation Runs with HYDRUS-1D

Initial tension (-330 and -4,000 H<sub>2</sub>O-cm) and profile layering pattern (Cún-1, Cún-2 and TML) significantly influenced the temporal changes in tension in the studied profiles. When initial tension was set to -330 H<sub>2</sub>O-cm, final tension values reached -2,800 to -12,500 H<sub>2</sub>O-cm on day 30 depending on

the observation depths (5, 10, 15, 20) and the daily evaporation rates (3, 5 and 7 mm d<sup>-1</sup>). Final tension values were below the tension threshold line of -2,000 H<sub>2</sub>O-cm (initial water stress) for all observation depths in profiles Cún-1 and TML (Fig. 4). A characteristic difference in hydraulic behaviour existed between profile Cún-2 and the other two profiles at depths of 15 and 20 cm, regardless of the daily evaporation rate. The Cún-2 tension time series reached the water-stress threshold value at the depths of 15 cm on day 27, while tension at a depth of 20 cm in profile Cún-2 did not reach the threshold of -2,000 H<sub>2</sub>O-cm. This behaviour was likely caused by the presence of the fine-textured topsoil in profile Cún-2.

When initial surface tension was set to -4,000 H<sub>2</sub>O-cm, tension time series at all depths and in all scenarios showed decreasing tension values (Figs 4j-r). Observation depths 10, 15 and 20 cm demonstrated a weak resistance against evapotranspiration. This tension value may be ideal during the final ripening phase of cereals (oat, wheat and rye) but insufficiently low during the early phenological phases of cereals, leguminous crops and vegetables. A tension of -15,000 H<sub>2</sub>O-cm was reached in 12 to 20 days after the onset of the simulation at a depth of 5 cm.

Final matric potential values were between -4,800 and -18,278 H<sub>2</sub>O-cm on day 30. The driest conditions on day 30 were reached in profile Cún-2 at a depth of 5 cm at a daily evaporation rate of 7 mm d<sup>-1</sup>. However, evapotranspiration rate had little effect on final tension values (Fig. 4) as tension values on day 30 at a depth of 5 cm ranged between 16,724 and 18,278 H<sub>2</sub>O-cm in profiles Cún-1 and Cún-2, respectively, for all three evapotranspiration scenarios. The limited influence of evapotranspiration on the temporal pattern on tension is likely explained by the fine-textured topsoil of all three simulated profiles. Secondly, the coarser texture of the topsoil in profile TML capillary rise must have been stopped at the boundary of the top 50 cm and the underlying horizon of finer texture. The tension time series therefore indicated no replenishment by capillary rise.

Although profile Cún-2 had a more profoundly multilayered character than Cún-1, in general, moisture contents more rapidly depleted in profile Cún-1 (at the depths of 15 and 20 cm) than in

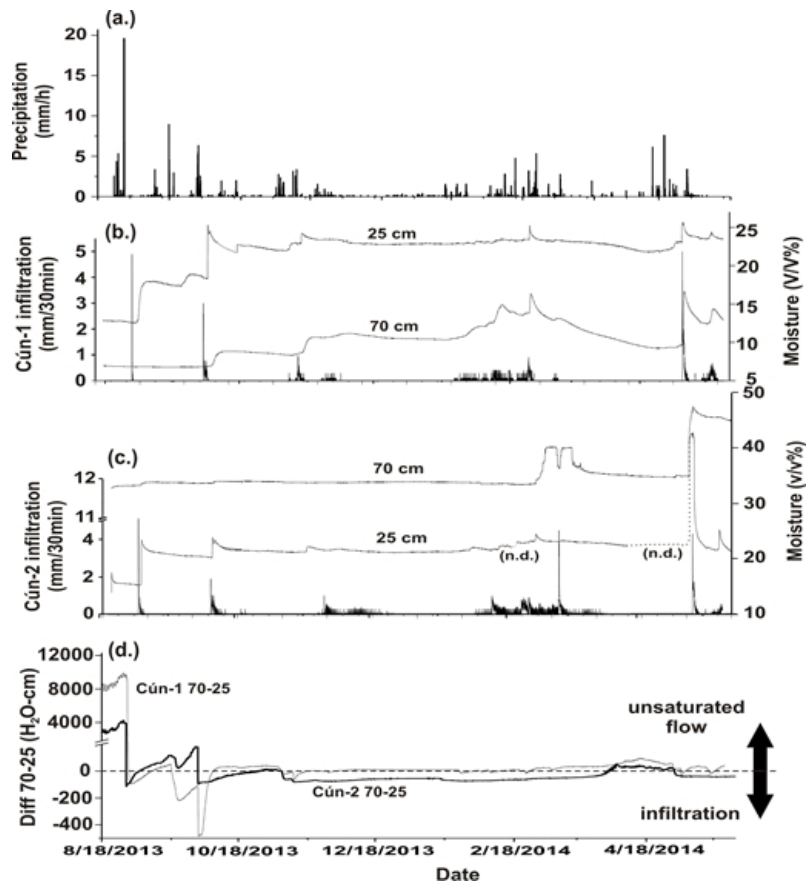


Fig. 3. Field monitoring of precipitation (a); infiltration at Cún-1 (b); infiltration at Cún-2 (c); and difference between water potential at 70 cm and 25 cm depths (d)

profile Cún-2 when initial tension was set to  $-330 \text{ H}_2\text{O-cm}$ . This is likely explained by the character of finer texture between 0 to 120 cm of the profile and therefore the higher retention capacity of the topsoil, especially due to the clay loam texture of the top 35 cm. The multilayered structure of Cún-2 retained water more efficiently than the more homogeneous profile of Cún-1. However, profile Cún-1 is less likely to be replenished by capillary rise from groundwater in the summer, due to the underlying coarse sandy layers. This observation confirms that large textural contrasts in the multilayered profile hinder upward moisture fluxes by capillary rise.

The initial tension parameter played a crucial role on the outcomes of the simulation of the 30-day meteorological drought. At the same time, evapotranspiration did not, or hardly, influenced model results, as final tension values demonstrated only small differences at the three input daily evapotranspiration rates. Similarly, the times when water-stress condition threshold values were reached

after the start of the simulations at the three evapotranspiration rates showed only minor differences. Although the textural profiles were the opposite for profiles Cún-1 (fine sediments underlain by coarse sediments) and TML (coarse sediments underlain by fine-textured material) simulation outcomes were characterised by similar patterns, while profile Cún-2 was drier than both profiles Cún-1 and TML. In other words, the number of horizons or layers with contrasting texture has a profound influence on the hydraulic properties of the profile of interest (Miller and White 1998; Huang et al. 2013).

### 3.4. Spatial distribution of DSAs

Although the AGROTOPO soil textural map generated for the topsoil (0 to 20 cm) effectively supports national-level decision making, it is only conditionally applicable to regional-scale management problems. In other words, it cannot be directly used to

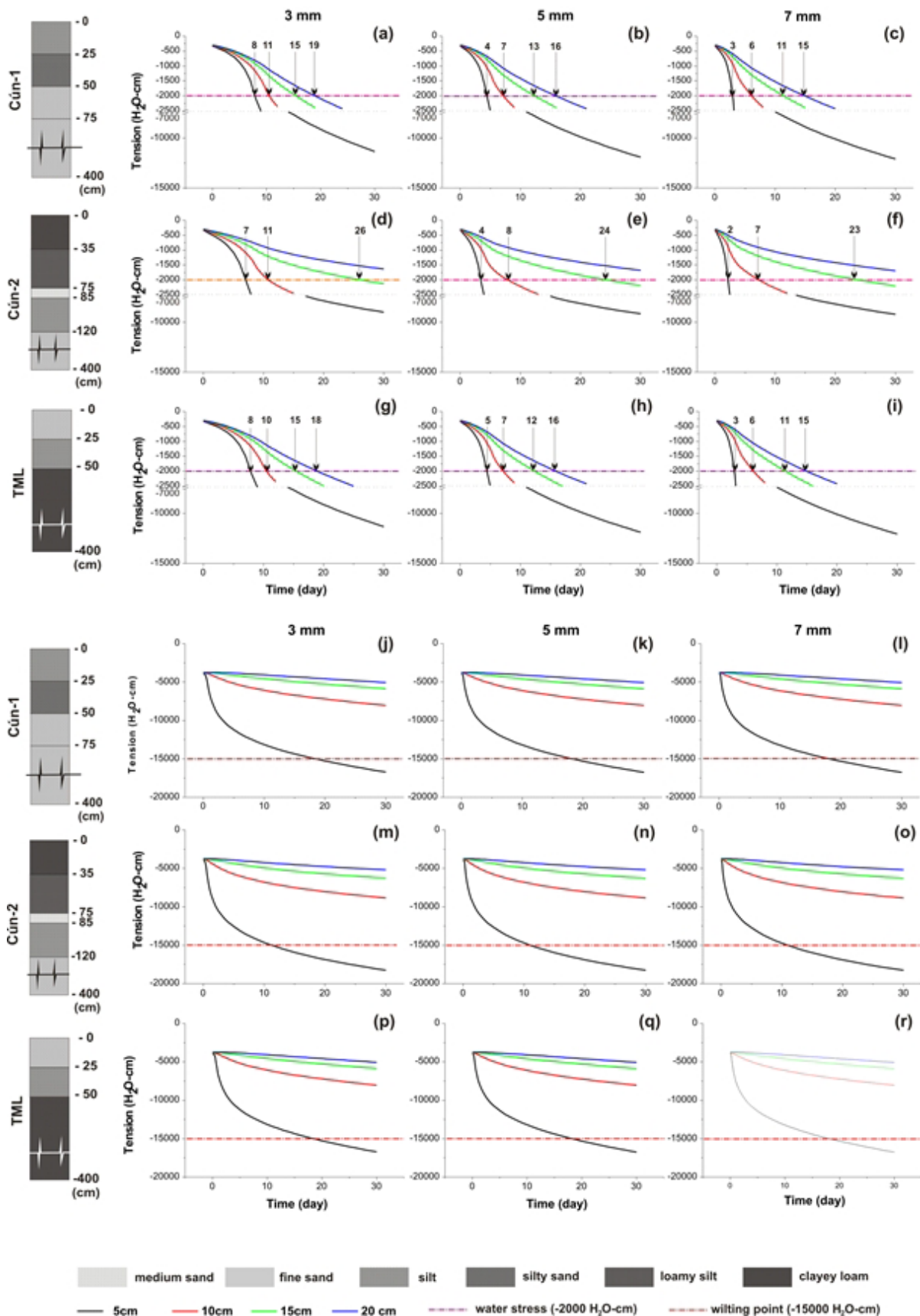


Fig. 4. Modelled tension time series for profiles Cún-1, Cún-2 and TML at daily evaporation rates of 3, 5 and 7 mm d<sup>-1</sup> and at initial surface tensions of -330 H<sub>2</sub>O-cm (a-i) and -4,000 H<sub>2</sub>O-cm (j-r); numbers on figures a to i indicate the number of days it took to reach the water stress threshold of -2,000 H<sub>2</sub>O-cm

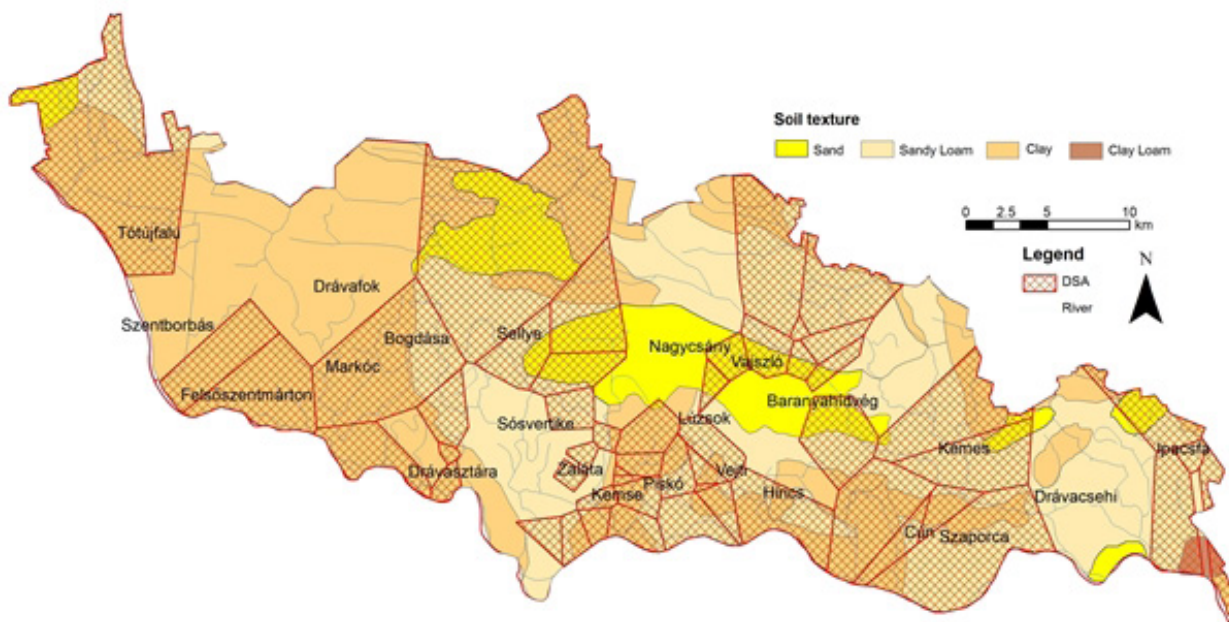


Fig. 5. Distribution of DSAs (indicated by red cross hatch) determined in the current study for the operational area of the Ancient Drava River and surface soil texture according to the AGROTOPO database

estimate the spatial distribution of drought hazard. To overcome the limited applicability of the AGROTOPO database, at least for the goals of the current study, we aimed to delineate the spatial distribution of drought-sensitive areas within the operational area of the ODP. Simulation of hydraulic properties with HYDRUS-1D indicated that the presence of contrasting textural properties and at least one sandy horizon increases an area’s drought sensitivity. To identify the spatial distribution of multilayered structures, which are associated with reduced vertical fluxes, we delineated areas where soil profiles are characterised by contrasting texture and include at least one sandy layer.

Sandy topsoil in the AGROTOPO database (only available for the surface) covered an area of 76.31 km<sup>2</sup>, i.e. 12.98% of the entire studied area. For the field-sampling-based DSA map the mean polygon size was 6.68 km<sup>2</sup>, the smallest polygon had a land area of 0.175 km<sup>2</sup> and the largest one covered a surface area of 82.6 km<sup>2</sup>. For the DSA<sub>0-20</sub> map, which was generated using the textural data of the 88 field-augered samples, sand was found in 9.52 % of the entire land area of the ODP, which corresponds well with the surface percentage of sand in the AGROTOPO database.

When sand percentage was determined for the depths of 0–20, 20–60 and 60–120, topsoil (0 to 20

cm) had the lowest fraction of sand. Increasing percentages of sand were found in layers 20–60 and 60–120. Sand was found in 24.93% and 51.72% for the depths of 20–60 and 60–120 cm, respectively. Overall, when all layers were considered in the three textural maps between the depths of 0 and 120 cm, DSAs covered 64.78% of the studied area.

### Conclusions

The current study aimed to determine the spatial distribution of areas potentially affected by drought in the floodplain of the River Drava, SW Hungary. To achieve this, we modelled whether capillary rise could contribute to the re-supply and replenishment of soil moisture in the root zone of rain-fed crops conventionally grown in the studied area.

As our HYDRUS-1D model simulations pointed out, capillary rise and upward movement of soil moisture is limited where capillary barriers are present at the interfaces between layers of contrasting soil textures. Similarly, the presence of layers of sandy texture may indicate reduced capillary rise due to the larger fraction of macropores (Campbell 1985). Infiltration and drainage processes in multi-layered soils are complicated by the contrast-

ing hydraulic properties (Huang et al. 2011). The spatial heterogeneity of soil texture therefore significantly influences water dynamics and replenishment, as well as the spatial distribution of drought hazard, even at a horizontal scale of a few metres. Multilayered soils often demonstrate poor hydraulic properties and weak suction due to the presence of capillary rise barriers (Campbell 1985). Other multilayered soils, however, due to the presence of capillary and hydraulic barriers, may hold more water than non-layered soils (Zettl et al. 2011; Li et al. 2013). Layers of sandy texture may decrease capillary rise (Campbell 1985), similarly to soils of very fine, clayey texture, where upward movement of water is retarded (Li et al. 2011). Loss of moisture may be significant due to evaporation to a depth of 60 cm in sandy soils (Hellwig 1973).

Our results may be inspiring in terms of understanding water dynamics of soils of heterogeneous hydraulic properties, but need to be handled with extreme caution with respect to drought hazard. Extreme subsurface heterogeneity was also revealed by field borehole sampling and profile excavations. Although the area has a relatively uniform macrotopography (slope gradients in the studied area are less than  $0.002 \text{ m m}^{-1}$  and relief differences are less than  $\pm 1 \text{ m km}^{-2}$ ), the fluvial processes and meandering character of the Drava River give the soil texture extreme spatial heterogeneity and, consequently, create a high-level of uncertainty in the assessment of rhizospheric soil moisture.

In summary, from our findings the following specific conclusions have been drawn:

1. The physical properties of soil in the studied floodplains are extremely heterogeneous due to random past sedimentation dynamics. Therefore, water availability, water retention and capillary rise in the shallow rhizosphere are significantly controlled by subsurface heterogeneity and stratification.
2. Although profile Cún-2 has a more contrasting textural character than Cún-1, depletion of moisture content was less pronounced in profile Cún-2 than in Cún-1. This was indicated with inverse soil moisture vertical distribution by the field data. Such an observation has already been confirmed by previous studies (e.g. Li et al. 2011).
3. According to HYDRUS-1D model runs, the more complex and more contrasting the subsurface horizonation in terms of soil texture, the more reduced the vertical water flux is within the profile. Multilayered structure had a more profound effect on the water dynamics of the root zone than daily evaporation rates.
4. HYDRUS-1D model runs indicated that capillary rise contributing to the water supply of the topsoil is reduced when major textural differences hinder the upward movement of soil moisture in the profile, triggering drought risk in the root zone.
5. Upscaling our results to floodplain scale and to a depth of 120 cm, drought likely affects 64% of the entire studied area.

The approach used in the current study can be applied to areas of Fluvisols along floodplains characterised by heterogeneous hydraulic properties and contrasting vertical textural properties under humid continental and maritime climates. Nonetheless, here we described homogeneous flow, whereas, in the field, preferential flow may also contribute to subsurface moisture conditions and solute pulses during individual rainstorms, as indicated by past studies, e.g. Hendrickx and Flury (2001) and Mulane et al. (2015).

Based on the distribution of DSAs, recommendations can be made for best farming practices. However, water stress has not only been observed for crops grown within the area of the ODP but also in the forests and woodlands of the Danube–Drava National Park, as indicated by reduced tree and sapling growth. Hence, to increase the spatial resolution of the moisture availability and detection of areas of water shortage, further analyses and additional field-collected or remotely-sensed datasets (e.g.  $K_s$ ,  $\theta_s$  and  $\theta_r$ ) are required. If a spatial resolution of a few tens of metres is achieved, that would already reflect the vegetational and morphological patterns of point bars and the moisture-characteristics of ridge-and-swale topography along the left-bank floodplain of the River Drava with sufficient detail.

The DSA maps with the integrated textural and model-based hydrodynamical details may provide a more detailed picture on the water dynamics of the Drava floodplain. The locations of DSA areas provide valuable information for stakeholders and lo-

cal farmers to implement appropriate management. At local levels, soil textural data derived from field surveys and upscaled by interpolation and incorporated into the existing soil databases could also increase the resolution and accuracy of national-scale soil maps (Laborczy et al. 2016, 2018).

## Acknowledgements

The authors are indebted to Gábor Horváth (DDVIZIG) for providing data to the current research. The authors are also grateful to the Hungarian National Scientific Fund (OTKA, contract number: K 104552), the project “Higher Education Institution Excellence” 20765/3/2018 FEKUTSTRAT (Topic 3/1, “Through innovation for sustainable and healthy life and environment) and the GINOP-2.3.2.15-2016-00055 research fund for financial support.

## Disclosure statement

No potential conflict of interest was reported by the authors.

## Author Contributions

Study design: J.D., S.C., G.N., E. P., M.S., D.L.; data collection J.D., S.C., G.N., E. P., M.S., D.L.; statistical analysis: J.D., S.C., G.N., E. P., M.S., D.L.; result interpretation J.D., S.C., G.N., E. P., M.S., D.L.; manuscript preparation J.D., S.C., G.N., E. P., M.S., D.L.; literature review: J.D., S.C., G.N., E. P., M.S., D.L.

## References

ARKHANGELSKAYA TA, KHOKHLOVA OS and MYAKSHINA TN, 2016, Mathematical modeling of water fluxes in arable chernozems under differ-

ent land use. *Eurasian Soil Science* 49:773–783, DOI: <https://doi.org/10.1134/S1064229316070024>.

- BRUCH PG, 1993, Laboratory study of evaporative fluxes in homogeneous and layered soils. M.Sc. thesis, Department of Civil Engineering, University of Saskatchewan, Saskatoon, SK.
- BURIÁN A, HORVÁTH G and MÁRK L, 2019, Channel Incision Along the Lower Drava. In: Lóczy D (ed.), *The Drava River: Environmental Problems and Solutions*. Springer Science + Media, Cham, Switzerland, 139–157.
- CAMPBELL GS, 1985, *Soil Physics with BASIC—Transport Models for Soil-Plant Systems*. Elsevier Co., Amsterdam. ISBN 9780080869827.
- COLLOFF M and BALDWIN SD, 2010, Resilience of floodplain ecosystems in a semi-arid environment. *The Rangeland Journal* 32(3): 305–314, DOI:10.1071/RJ10015.
- DEZSŐ J, LÓCZY D, SALEM AM and NAGY G, 2018, Floodplain connectivity. In: Lóczy D (ed.), *The Drava River: Environmental Problems and Solutions*. Springer Science + Media, Cham, Switzerland, 215–230.
- EUROPEAN PARLIAMENT, 2008, Climate change-induced water stress and its impact on natural and managed ecosystems. Study for the European Parliament Committee on Environment, Public Health and Food Safety. IP/A/ENVI/FWC/2006-172/LOT1/CI/SC12). [https://www.ecologic.eu/sites/.../SC\\_12\\_Climate\\_induced\\_Water\\_Stress\\_Jan\\_2008.pdf](https://www.ecologic.eu/sites/.../SC_12_Climate_induced_Water_Stress_Jan_2008.pdf) (accessed 20.02.2018).
- FAO, 2012, Crop yield response to water. FAO Irrigation and Drainage Paper 66, Rome. <http://www.fao.org/docrep/016/i2800e/i2800e.pdf> (last accessed on February 21, 2018).
- FLINT AL, FLINT LE, 2002, Particle density. In: Dane JH and Topp GC (eds), *Methods of soil analysis: Part 4. Physical methods*. SSSA Book Ser. 5. SSSA, Madison, WI, 229–240.
- GAO Y, DUANA A, QIUA X, LIUA Z, SUNA J, ZHANGA J and WANGA H, 2010, Distribution of roots and root length density in a maize/soybean strip intercropping system. *Agricultural Water Management* 98: 199–212, DOI: <https://doi.org/10.1016/j.agwat.2010.08.021>.
- GIBLING MR and RUST BR, 2009, Alluvial Ridge-and-Swale Topography: A Case Study from the Morien Group of Atlantic Canada. In: Marzo M and Puigdefábregas C (eds), *Alluvial Sedimentation*. The In-

- ternational Association of Sedimentologists. DOI: 10.1002/9781444303995.ch11.
- GOHARDOUST M, SADEGHI R, ZIATABAR M, AHMADI M, JONES SB and TULLER M, 2017, Hydraulic conductivity of stratified unsaturated soils: Effects of random variability and layering. *Journal of Hydrology* 546: 81–89. DOI: <http://dx.doi.org/10.1016/j.jhydrol.2016.12.055>.
- GROSSMAN RB and REINSCH TG, 2002, Bulk Density and Linear Extensibility: Core Method. In: Dane JH, Topp GC (eds), *Methods of Soil Analysis*. Part 4, Physical Methods, SSSA, Incorporated, Madison, 208–228.
- HELLWIG HR, 1973, Evaporation of water from sand, 3: The loss of water into the atmosphere from a sandy river bed under arid climatic conditions. *Journal of Hydrology* 18: 3–4.
- HENDRICKX JMH and FLURY M, 2001, Uniform and preferential flow mechanisms in the vadose zone. In: National Academy Council, editor. *Conceptual models of flow and transport in the fractured vadose zone*. National Academy Press, Washington DC. 149–187.
- HUANG M, BARBOUR SL, ELSHORBAGY A, ZETTL JD and SI BC, 2011, Infiltration and drainage processes in multilayered coarse soils. *Canadian Journal Soil Science* 91: 169–183.
- HULISZ P, MICHALSKI A, DĄBROWSKI M, KUSZA G and ŁĘCZYŃSKI L, 2015, Human-induced changes in the soil cover at the mouth of the Vistula River Cross-Cut (northern Poland). *Soil Science Annual* 66: 67–74.
- IUSS Working Group WRB, 2015, World Reference Base for Soil Resources 2014, update 2015 International soil classification system for naming soils and creating legends for soil maps. World Soil Resources Reports No. 106. FAO, Rome.
- KARASIEWICZ TM, HULISZ P, NORYSKIEWICZ AM and STACHOWICZ-RYBKA R, 2017, Post-glacial environmental history in NE Poland based on sedimentary records from the Dobrzyń Lakeland. *Quaternary International* 1–15. DOI: <https://doi.org/10.1016/j.quaint.2017.10.039>
- KARUP D, MOLDRUP P, TULLER M, ARTHUR E and DE JONGE LW, 2016, Prediction of the soil water retention curve for structured soil from saturation to oven-dryness. *European Journal of Soil Science* 68: 57–65, DOI: 10.1111/ejss.12401.
- KISS A and NIKOLIĆ Z., 2015, Droughts, Dry Spells and Low Water Levels in Medieval Hungary (and Croatia) I: The Great Droughts of 1362, 1474, 1479, 1494 and 1507. *Journal of Environmental Geography* 8 (1–2), 11–22. DOI: 10.1515/jengeo-2015-0002.
- LABORCZI A, SZATMÁRI G, KAPOSÍ AD and PÁSZTOR L, 2018, Comparison of soil texture maps synthesized from standard depth layers with directly compiled products. *GEODERMA*, DOI: <https://doi.org/10.1016/j.geoderma.2018.01.020>.
- LABORCZI A, SZATMÁRI G, TAKÁCS K and PÁSZTOR L, 2016, Mapping of topsoil texture in Hungary using classification trees. *Journal of Maps* 12:(5) 999–1009.
- LI X, CHANG SX and SALIFU FK, 2013, Soil texture and layering effects on water and salt dynamics in the presence of a water table: a review. Published at [www.nrcresearchpress.com/er](http://www.nrcresearchpress.com/er) on 19 August 2013.
- LIEB GK and SULZER W, 2019, Land Use in the Drava Basin: Past and Present: Environmental Problems and Solutions. In: Lóczy D (ed.), *The Drava River: Environmental Problems and Solutions*. Springer Science + Media, Cham, Switzerland, 27–45.
- LIZASO JI and RITCHIE JT, 1997, Maize shoot and root response to root zone saturation during vegetative growth. *Agronomy J.* 89: 125–134.
- LÓCZY D, 2019, Climate and climate change in the Drava-Mura catchment. In: LÓCZY D (ed.), *The Drava River: Environmental Problems and Solutions*. Springer Science + Media, Cham, Switzerland, 45–61.
- LÓCZY D, DEZSŐ J, CZIGÁNY SZ, PROKOS H and TÓTH G, 2017, An environmental assessment of water replenishment to a floodplain lake. *Journal of Environment* 202: 337–347, DOI: <http://dx.doi.org/10.1016/j.jenvman.2017.01.020>.
- LÓCZY D and DEZSŐ J, 2019, Landscape Rehabilitation: The Old Drava Programme: Environmental Problems and Solutions. In: Lóczy D (ed.), *The Drava River: Environmental Problems and Solutions*. Springer Science + Media, Cham, Switzerland, 367–393.
- LÓCZY D, DEZSŐ J, GYENIZSE P, CZIGÁNY SZ and TÓTH G, 2019, Oxbow lakes: Hydromorphology. In: Lóczy D (ed.), *The Drava River: Environmental Problems and Solutions*. Springer Science + Media, Cham, Switzerland, 177–199.
- MAKÓ A, TÓTH B, HERNÁDI H, FARKAS CS and MARTH P, 2010, Introduction of the Hungarian Detailed Soil Hydrophysical Database (MARTHA)

- and its use to test external pedotransfer functions. *Agrokémia és Talajtan*. 59: 29–38. DOI: <http://dx.doi.org/10.1556/Agrokem.59.2010.1.4>.
- MAMEDOV AI, EKBERLI I, GÜLSER C, GÜMÜŞ I, ÇETİN U and LEVY GJ, 2016, Relationship between soil water retention model parameters and structure stability. *Eurasian Journal of Soil Science* 5: 255–331, DOI: 10.18393/ejss.2016.4.314-321.
- MILLER DA and WINTER RA, 1998, A Conterminous United States Multilayer Soil Characteristics Dataset for Regional Climate and Hydrology Modeling. *Earth Interactions* 2: 2 1–25.
- MOHAWESH O, JANSSEN M, MAAITAH O and LENNARTZ B, 2017, Assessment the effect of homogenized soil on soil hydraulic properties and soil water transport. *Eurasian Soil Science* 50: 1077–1085, DOI: <https://doi.org/10.1134/S1064229317090046>.
- MUALEM Y, 1976, A new model for predicting the hydraulic conductivity of unsaturated porous media. *Water Resources Reseach* 12: 513–522, DOI:10.1029/WR012i003p00513.
- MULLANE JM, FLURY M, IQBAL H, FREEZE PM, HINMAN C, COGGER CG and SHI Z, 2015, Intermittent rainstorms cause pulses of nitrogen, phosphorus and copper in leachate from compost in bioretention systems. *Science of the Total Environment*. 537: 294–303, DOI:10.1016/j.scitotenv.2015.07.057.
- PIRKHOFFER E, CZIGÁNY SZ, GYENIZSE P and NAGYVÁRADI L, 2006, A meteorológiai modellek talajadatbázisainak összehasonlító elemzése. In: III. Magyar Földrajzi Konferencia. Absztrakt kötet. MTA Földrajztudományi Kutatóintézet, Budapest, p. 178.
- RAJKAI K and KABOS S, 1999, A talaj víztartóképeség-függvény (pF-görbe) tulajdonságok alapján történő becslésének továbbfejlesztése. *Agrokémia és Talajtan* 48: 15–32.
- RAJKAI K, TÓTH B, BARNA GY, HERNÁDI H, KOC SIS M and MAKÓ A, 2015, Particle-size and organic matter effects on structure and water retention of soils. *Biologia*. 70: 1456–1461, DOI: <http://dx.doi.org/10.1515/biologia-2015-0176>.
- Si B, Dyck M and Parkin GW, 2011, Flow and transport in layered soil preface. *Canadian Journal of Soil Science* 91(2): 127, DOI: 10.4141/cjss11501.
- ŠIMŮNEK J, SEJNA M, SAITO H, SAKAI M and VAN GENUCHTEN MTh, 2008, The HYDRUS-1D Software Package for simulating the one-dimensional movement of water, heat, and multiple solutes in variably saturated media. Version 4.08. HYDRUS Software Series 3, Department of Environmental Sciences, University of California Riverside, Riverside, California, USA.
- ŠIMŮNEK J, VAN GENUCHTEN MTh and ŠEJNA M, 2016, Recent developments and applications of the HYDRUS computer software packages. *Vadose Zone Journal* 15, DOI: 10.2136/vzj2016.04.0033.
- SŁOWIK M, DEZSŐ J, MARCINIÁK A, TÓTH G and KOVÁCS J, 2018, Evolution of river planforms downstream of dams: Effect of dam construction or earlier human-induced changes? *Earth Surface Processes and Landforms* 43: 2045–2063.
- THORNTHWAITTE CW, 1948, An approach toward a rational classification of climate. *Geographical Review* 38: 5–94.
- TÓTH B, WEYNANTS M, NEMES A, MAKÓ A, BILAS G and TÓTH G, 2015, New generation of hydraulic pedotransfer functions for Europe. *European Journal of Soil Science* 66: 226–238, DOI: 10.1111/ejss.12192.
- VAN GENUCHTEN MTh, 1980, A closed-form equation for predicting the hydraulic conductivity of unsaturated soils. *Soil Science Society of America Journal* 44: 892–898.
- VAN GENUCHTEN MTh, LEIJ FJ and YATES SR, 1991, The RETC code for quantifying the hydraulic functions of unsaturated soils Version 1.0. EPA Report 600/2-91/065, U.S. Salinity Laboratory, USDA, ARS, Riverside, CA. <https://www.pc-progress.com/Documents/programs/retc.pdf> (last accessed on February 26, 2018).
- VÁRALLYAY GY and RAJKAI K, 1987, Soil moisture content and moisture potential measuring techniques in Hungarian soil survey. In: Proc. of Int. Conf. on 'Measurement of Soil and Plant Water Status' Vol. 1. July 6–10, 1987. Logan, UT, 183–184.
- VÁRALLYAY GY, SZŰCS L, MURÁNYI A, RAJKAI K and ZILAHY P, 1979, Magyarország termőhelyi adottságait meghatározó talajtani tényezők I:100 000 térképe I. *Agrokémia és Talajtan* 28: 363–384.
- VÁRALLYAY GY, SZŰCS L, MURÁNYI A, RAJKAI K and ZILAHY P, 1980, Magyarország termőhelyi adottságait meghatározó talajtani tényezők I:100 000 térképe II. *Agrokémia és Talajtan* 29: 35–76.
- VERECKEN H, SCHNEPF A, HOPMANS JW, JAVAUX M, OR D, ROOSE T, VANDERBORGH T, YOUNG MH, AMELUNG W, AITKENHEAD M, ALLISON SD, ASSOULINE S, BAVEYE P, BERLI M, BRÜGGEMANN N, FINKE P, FLURY M, GAISER T, GOVERS G, GHEZZEHEI T, HALLETT P, HEN-

- DRICKS HJ, FRANSSSEN J, HEPPELL J, HORN R, HUISMAN JA, JACQUES D, JONARD F, KOLLET S, LAFOLIE F, LAMORSKI K, LEITNER D, MCBRATNEY A, MINASNY B, MONTZKA C, NOWAK W, PACHEPSKY Y, PADARIAN J, ROMANO N, ROTH K, ROTHFUSS Y, ROWE EC, SCHWEN A, ŠIMŮNEK J, TIKTAK A, VAN DAM J, VAN DER ZEE SEATM, VOGEL HJ, VRUGT JA, WÖHLING T and YOUNG IM, 2016, Modeling soil processes: Review, key challenges, and new perspectives. *Vadose Zone Journal* 15: 5, 1–57, DOI: 10.2136/vzj2015.09.0131.
- VOGT JV and SOMMA F, 2013, Drought and Drought Mitigation in Europe. Springer Science & Business Media, Dordrecht, Netherlands. ISBN 9789048155682.
- WINTER TC, HARVEY JW, FRANKE OL and ALLEY WM, 1999, Groundwater and surface water: A single resource. *U.S. Geological Survey Circular* 1139: 1–79.
- ZETTL JD, BARBOUR SL, HUANG M, SI BC and LESKIW LA, 2011, Influence of textural layering on field capacity of coarse soils. *Canadian Journal of Soil Science* 91: 133–147.

Received 11 September 2018

Accepted 20 May 2019